Photorefractive Materials for Nonvolatile Volume Holographic Data Storage

Lambertus Hesselink,*† Sergei S. Orlov, Alice Liu, Annapoorna Akella, David Lande, Ratnakar R. Neurgaonkar

Optically gated recording and nonvolatile readout in a digital volume holographic data storage system that uses a pair of mutually incoherent light sources during recording and only one for readout were demonstrated recently. This approach used stoichiometric lithium niobate, which after post-growth processing gave rise to an at least two orders of magnitude improvement in sensitivity over the best materials reported previously. It is also shown that by adding certain dopants (iron and manganese) to near-stoichiometric lithium niobate, the dark storage time and gating efficiency can be increased compared with previous work. The underlying physical mechanisms of gated recording and the effectiveness of the gating process responsible for this manifold improved performance are discussed, and bipolarons and small polarons are identified as the responsible photorefractive species.

Holographic data storage systems have long held promise for their high storage capacity, short access times, and high data transfer rates. Photorefractive materials such as lithium niobate ($LiNbO_3$) can be used to record holograms with modest laser power (Fig. 1).

Illumination of a spatially varying light pattern, such as from the superposition of two mutually coherent plane waves, stimulates a charge distribution that gives rise to a corresponding change in the index of refraction of the medium through the electrooptic effect (*1*). Although several undoped ferroelectric media exhibit a photorefractive response, the strength of the effect can be improved by orders of magnitude by adding selected dopants to the medium during crystal growth. For example, iron (Fe) is a well-known dopant in congruent $LiNbO_3$ [when $LiNbO_3$ is grown by melting Li_2CO_3 and Nb_2O_5, the congruently melting composition is 48.6 mole percent (mol %) Li_2O, as opposed to 50 mol % for stoichiometric $LiNbO_3$]. Iron is present in the crystal as Fe^{2+} and Fe^{3+}, in a ratio determined by post–crystal growth annealing in an oxidizing or reducing atmosphere. The Fe^{2+} acts as a donor ion, which upon absorption of a photon produces an electron and Fe^{3+}, which acts as an acceptor for free carriers. The free electrons move in the crystal from regions of intense illumination to darker areas under diffusion, drift, or photovoltaic forces. The free electrons are captured by the acceptors, reducing Fe^{3+} into Fe^{2+}. Through repeated steps, electrons tend to be trapped by Fe^{3+} ions in regions where the light intensity is low. The charge redistribution gives rise to a spatially varying electric space charge field that changes the index of refraction of the material locally through the electrooptic effect and represents the holographic information to be stored. Upon readout of the hologram, the stored information is retrieved but also erased because the medium remains photosensitive. The readout beam, which usually is a uniform plane wave, excites free electrons again and redistributes the charges uniformly throughout the recording medium.

For holographic storage applications, erasure upon readout is usually (but not always) undesirable, and much work has been expended to find a fixing process similar to that for photographic film, but without the need for chemical processing. Several techniques have been developed for this purpose, including thermal and electrical fixing, and system approaches based on refreshing the memory have been suggested as well.

As an alternative procedure, early work in the 1970s focused on the use of an additional light source during the recording process that is not present during readout (*2*). This light source can be incandescent and does not have to be coherent. The material is sensitive to the writing wavelength only in the presence of gating or bias light, whereas it is insensitive to readout light by itself. This optically induced light sensitivity is potentially a very attractive mechanism for data recording and readout; it allows long-term storage and virtually nondestructive readout.

In early work, pulsed lasers were used to achieve large intensities to take advantage of optical nonlinearities. Transition metals were doped into a variety of host materials, including $LiNbO_3$, potassium tantalate-niobate, and lithium tantalate ($LiTaO_3$). Experiments showed that by the use of a fundamental harmonic (1.064 m) of a yttrium-aluminum-garnet laser for writing the data and its second harmonic (532 m) for gating, long erasure times could be obtained, but the required near infrared (IR) intensities were on the order of 10^8 W/cm^2 (*2*). For practical applications, low-power continuous-wave (CW) lasers are needed. In recent years, there has been renewed interest in this work, with advances being made with the use of rare Earth elements doped into ferroelectric materials (*3*). Although it was thought at the time that the rare Earth dopants were responsible for the observed increased sensitivity of two-photon recording, we found this not to be the case. In addition, these previous studies achieved gated recording sensitivities still one to two orders of magnitude lower than nongated recording sensitivities for Fe-doped $LiNbO_3$ materials with green light. These sensitivities are too small for practical use. In fact, the CW experiments with rare Earth doped materials are generally of similar sensitivity as the pulsed experiments, and the total absorbed energy is about the same.

To characterize the sensitivity of a medium, we developed several measures that generally relate the measured diffraction efficiency or the index of refraction change under illumination to the incident light intensity. We define the recording sensitivity S for gated recording as

$$S = \frac{\partial \sqrt{\eta}}{\partial t} \frac{1}{I_{IR} L} \quad (1)$$

where η is the diffraction efficiency, L is the thickness of the medium, t is time, and I_{IR} is the CW recording intensity. Typical values of S for

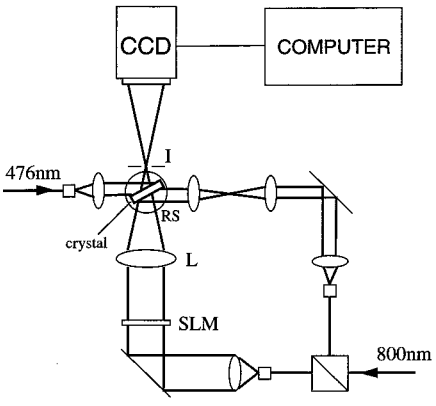

Fig. 1. Optical setup for digital holographic recording. Phase conjugate readout is achieved by rotating the crystal 180° around the vertical axis. CCD, charge-coupled device; L, lens; I, iris; RS, rotation stage; SLM, spatial light modulator.

L. Hesselink, A. Liu, A. Akella, D. Lande, Stanford University, Stanford, CA 94305, USA. S. S. Orlov, Optitek, 1330 West Middlefield Road, Mountain View, CA 94043, USA. R. N. Neurgaonkar, Rockwell International Science Center, 1049 Camino dos Rios, Thousand Oaks, CA 91360, USA.

*To whom correspondence should be addressed. E-mail: bert@kaos.stanford.edu
†All authors contributed equally to this work.

Fe-doped $LiNbO_3$ are from 0.02 to 0.10 cm/J, and it is mainly determined by the absorption coefficient of the recording light and the transport length of the excited carriers.

We recently reported (*4*) a digital holographic storage system that uses the two-photon gated recording method. Using a CW titanium: sapphire (800 nm) laser for writing and blue (476 nm) light for gating, we achieved high diffraction efficiency (several percent) and a low bit error rate (BER) ($<10^{-4}$) for a data mask image with 512 by 512 pixels. An undoped lightly reduced lithium niobate crystal of 49.6 mol % Li_2O composition with a maximum two-photon sensitivity of 0.01 cm/J (for a gating blue light intensity of about 0.2 W/cm^2) was used. The emphasis of that work was on the digital recording method with a gated recording scheme. We now discuss in detail the underlying physical mechanism for gated recording and the optimization of the medium properties and provide a method for substantial improvement over our earlier results. The key idea for optimization is to modify the host composition and the reduction state of the crystalline material (*5*). A surprising result is that the two-photon sensitivity has a sharp threshold (at about $[Li_2O] = 49.6$ mol %) dependence on the material composition near stoichiometry. (In past work on $LiNbO_3$, the congruent composition was chosen, because it provides the best optical quality crystals and because in single-photon recording the composition of the material is inconsequential.) Additionally, the gated two-photon sensitivity can be further increased through postgrowth reduction processing by a factor of at least 20 for undoped material. This procedure allowed us to achieve at least two orders of magnitude improved results over the best previous media for gated two-photon recording, making the two-photon sensitivity for near-IR light similar to the one-photon sensitivity of Fe-doped $LiNbO_3$ in the green region of the spectrum (in the near IR, Fe-doped $LiNbO_3$ is not sensitive for direct one-photon recording).

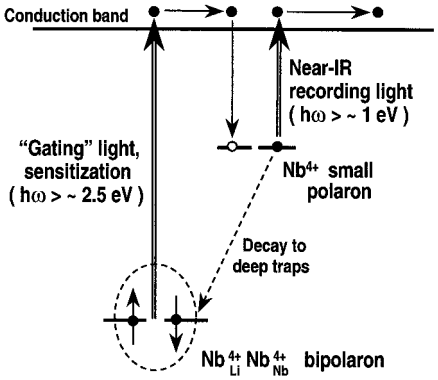

Fig. 2. Mechanism of optically gated recording in lithium niobate crystals. *h*, Planck's constant; ω, angular frequency.

Near the stoichiometric composition, intrinsic defects (bipolarons induced by reduction) are primarily responsible for the improved (up to 20 times compared with as-grown) gated recording sensitivity in undoped materials. However, further improvement in two-photon sensitivity is difficult to achieve because of rapid increase in the dark conductivity with even stronger reduction of undoped material. By adding appropriate donor dopants with energy levels similar to or deeper than corresponding levels of bipolarons, we can further increase the sensitivity without inducing a substantial dark conductivity. We investigated the impact of several extrinsic dopants (transition metal ions such as $Mn^{2+/3+}$ and $Fe^{2+/3+}$) on the two-photon recording process. We found that, under certain restricted conditions, both the two-photon sensitivity and the dark storage times can be simultaneously improved by optimizing the total concentration and the reduction state of the dopants. This process allowed us to design two-photon sensitive materials with both higher sensitivity (~0.03 cm/J) and larger gating efficiency (which is defined as the ratio of erasure rates for reading with and without gating beams) compared with nominally undoped materials.

The materials with large gated two-photon sensitivity have an additional advantage over Fe-doped congruent $LiNbO_3$ in that a strong light-induced absorption occurs during writing, but no or little absorption occurs while reading, which thereby reduces the absorption of the diffracted signal, giving rise to stronger diffracted signals.

The last advantage is related to optical damage in light-sensitive materials. When these media are exposed to more and more light, not only is the desired information recorded, but low spatial frequency index variations invariably occur as well. These variations are frequently referred to as optical damage, as these changes induce optical wavefront aberrations that tend to distort the optical illumination beam and they can even break it up into speckled intensity patterns. In Fe-doped $LiNbO_3$, the damage is proportional to the photovoltaic force, which in turn is proportional to the concentration of Fe^{3+} ions. This damage frequently limits the usable dynamic range of the material and storage capacity of Fe-doped $LiNbO_3$, long before other system limits such as cross talk between superimposed holograms become important. From a sensitivity and dynamic range point of view, it is desirable to control both the Fe^{2+} and Fe^{3+} concentrations through both postgrowth oxidation-reduction processing and total doping. Such control will give rise to both a high sensitivity (which is proportional to $[Fe^{2+}]$) and an optimal value of dynamic range (which is proportional to $[Fe^{3+}]$). Because of the optical damage limitations in one-photon recording schemes, a total dopant concentration ($[Fe^{2+}] + [Fe^{3+}]$) far below the value for maximum capacity is often necessary.

As a substantial advantage, in gated two-photon recording, the photovoltaic damage is also reduced by orders of magnitude because of very little single-photon absorption in the near IR during the readout (although for recording, some residual photovoltaic effect is present even in undoped $LiNbO_3$).

From the above discussion, it is apparent that several trade-offs between materials and system properties must be considered to achieve optimal performance. We will discuss the underlying physical mechanisms of gated recording, identify bipolarons and small polarons as the responsible photorefractive species, and describe the material modification methods responsible for substantially improved performance.

Materials Optimization: Undoped Lithium Niobate

Most of the previous work on gated two-photon recording has been carried out with congruent $LiNbO_3$, in doped or undoped form. The best results reported today in these materials have sensitivities at least two orders of magnitude less (*2*, *3*) than the results we now report. Such sensitivity is too small to store multiple digital data pages in the same volume with recording light intensities of 10 to 100 W/cm^2. A sensitivity of at least 0.01 cm/J is needed with a gating light intensity of less than 1 W/cm^2.

To achieve optically gated recording, there must be (i) deep traps that are partially filled with electrons to generate excited carriers during gating and recording of the hologram and (ii) shallow levels to trap photogenerated electrons, with sufficiently long lifetimes (hundreds of milliseconds) to absorb light at the writing wavelength. Intrinsic defects of lithium niobate represent a convenient scheme to realize two-photon gated recording. Lithium niobate crystals are in general not stoichiometric, as the chemical formula is given by $Li_{1-x}Nb_{1+x/5}O_3$ (and $x = 0.028$ for congruently melting material). Intrinsic point defects include Nb_{Li} (that is, a niobium ion on the Li site) antisite defects: $Nb_{Li}V_{Nb}$ and $Nb_{Li}Nb_{Nb}$ (*6*). The latter represents a two-electron trap or, when filled with a pair of electrons with opposite spins, a diamagnetic bipolaron $Nb^{4+}Nb^{4+}$. Illumination with blue-green light dissociates the bipolarons, and these electrons enter the conduction band and become self-trapped on the Nb lattice sites, forming Nb^{4+} small polarons (Fig. 2) (*7*). Small polaron levels can be viewed as shallow traps with a limited electron lifetime. For small polarons, the absorption due to optical excitation (hopping between different sites) is very broadband and peaks in the near IR region of the spectrum at

about 780 nm, which is twice the binding energy of polarons (0.8 eV). The photoexcitation by recording with near IR light and subsequent carrier redistribution and migration create the index hologram. The lifetime of the excited Nb^{4+} states depends on the density, capture cross section, and the reduction state of the deep defects, the temperature, and the intensity of the recording IR light. When the gating light is shut off, the carriers are eventually trapped in the deep traps, and the material is essentially transparent and not sensitive to near IR readout radiation, thus avoiding erasure, photoinduced scattering, and optical damage.

Optimization of the undoped crystalline material can be achieved through changing its stoichiometry and the reduction state (*5*, *8*) (Fig. 3 and Table 1). The gated photosensitivity of the material to near IR light is proportional to the density of excited small polarons and, therefore, is proportional to their recombination lifetime. High defect densities, as occur in congruent lithium niobate (48.6 mol % Li_2O), result in substantial lattice disorder and fast, nonradiative, phonon-assisted decay of Nb^{4+} polaron levels into deep traps and their recombination to bound bipolarons (*6*). As the material becomes closer to stoichiometric and the defect density decreases, the two-photon sensitivity S exhibits a sharp, two orders of magnitude increase with increased Li/Nb ratio up to 49.6 mol %, and then S saturates (Fig. 3). The lifetime of the upper Nb^{4+} levels in lithium niobate at room temperature changes from <40 ms for the congruent composition to ~400 ms for as-grown lithium niobate with a lower intrinsic defect density [with $x = 0.01$ (*3*)].

Similar threshold behavior with respect to composition has been observed in other phenomena that are related to the crystal defect structure of lithium niobate. For example, the ultraviolet-induced low-temperature luminescence due to electron hole recombination is almost completely quenched in lithium niobate with a high degree of lattice disorder (for example, congruently melting material) through nonradiative decay due to lattice defects and exhibits a step increase by two orders of magnitude for near-stoichiometric material with $[Li_2O] > \sim 49.6$ mol % in the crystal (*9*). The mechanism involved is the crystal lattice hardening due to decreased density of Nb_{Li} defects, which results in weak electron-phonon coupling and slower relaxation in near-stoichiometric material above the composition threshold, as opposed to strong electron lattice coupling and strong lattice relaxation in material with more intrinsic defects (*10*). Also, the total density of the $Nb_{Li}Nb_{Nb}$ defect sites that contain pairs of adjacent Nb ions in the same crystal cell, that is, the sites on which polarons are recombined forming bipolarons in lithium niobate (*6*), is decreased in near-stoichiometric material. For as-grown material, the increase in the small polaron lifetime achieved in near-stoichiometric lithium niobate results in about an order of magnitude improvement in the two-photon sensitivity ($\sim 10^{-3}$ cm/J) but still far below the one-photon sensitivity of Fe-doped congruent $LiNbO_3$ in the green.

Postgrowth reduction of near-stoichiometric crystals produces more filled bipolaron sites, which provide efficient absorption for the gating light of the blue-green region of the spectrum. Also, reduction converts the contaminant acceptor ions into donors (for example, Fe^{3+} into Fe^{2+}) that decrease the small polarons' capture cross section and increase their lifetime and, therefore, the material sensitivity under similar gating conditions. The lifetime of small polarons in optimally reduced crystals can be as long as several seconds and depends on the degree of reduction. More excessive reduction, however, results in very long polaron density lifetimes (tens of seconds) that adversely affect recording, in that the holograms exhibit a substantial dark decay right after writing.

Reduction of lithium niobate at high temperatures (900° to 1000°C) involves the migration of lithium vacancies from the bulk to the surface of the material (with corresponding back transport of free electrons for charge compensation). As a result, there is a surface reaction that involves a consumption of nonstoichiometric cells and generation of free electrons ($\bar{e}$) (*11*):

$$2(Nb_{Li}^{5+}V_{Nb}^{5-})^{1-}O_3 \rightarrow \tfrac{1}{2}\,O_2 \uparrow + (Nb_{Li}^{5+}Nb_{Nb}^{5+})^{4+}O_3 + V_{LiNbO_3} + 6\bar{e} \quad (2)$$

At lower temperatures, free electrons are trapped on the defect sites forming bipolarons, whereas charge compensation is still maintained by a change of the density of lithium vacancies:

$$(Nb_{Li}^{5+}Nb_{Nb}^{5+})^{4+} + 2\bar{e} \rightarrow (Nb_{Li}^{4+}Nb_{Nb}^{4+})^{2+} \quad (3)$$

A substantial increase in the blue-green absorption is seen in the reduced materials (Fig. 4). After the reduction, the two-photon photosensitivity of near-stoichiometric material improves by a factor of ~20 compared with as-grown materials (*5*). For undoped materials, the sensitivity saturates (or even decreases) for near-stoichiometric compositions with $[Li_2O] > 49.65$ mol %. Because the density of the defects ($Nb_{Li}Nb_{Nb}$) decreases as the composition becomes closer to exactly stoichiometric, the absorption of the gating light (and, hence, two-photon sensitivity) becomes somewhat smaller for more stoichiometric reduced crystals (Figs. 3 and 4). The saturation index change (that is, dynamic range), however, continues to grow with decreasing defect density.

Both sensitivity and the index change are enhanced in crystals with increased bipolaron concentration (Fig. 3). In the presence of the gating light, the induced absorption at the recording near IR wavelength (800 nm) is on the order of 0.1 cm^{-1}. Without gating, the erasure upon readout and IR one-photon sensitivity is determined essentially by a self-gating process that is due to the absorption tail of deep impurities in the near IR. The sensitivity of the material is at least 50 times less and therefore allows readout of the hologram thousands of times before substantial erasure takes place (Fig. 5). Dark decay of the hologram is determined by thermally induced electrons from deep bipolaron sites into the conduction band. Currently, the room tem-

Table 1. Determination of the stoichiometry of $LiNbO_3$ with phase-matching temperatures (T_{pm}) for crystals of various starting compositions [see (*8*)].

Li_2O (mol %) in melt	Li_2O (mol %) in crystal	T_{pm} (°C)
48.6	48.6	<room temperature
50	49.3	118
53	49.6	152
54	49.7	165
56	49.8	197
57	49.9	213
58	49.9	227

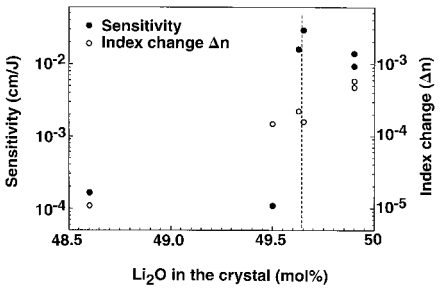

Fig. 3. Gated photosensitivity and index change versus material composition (Li content). All crystals are partially reduced. Gating intensity is 0.25 W/cm^2 at 457.9 nm.

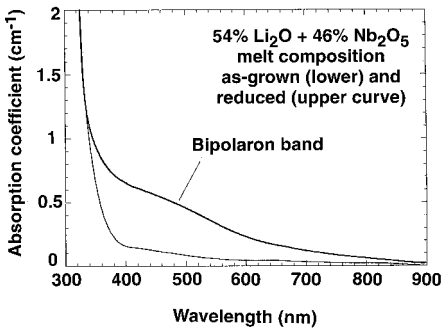

Fig. 4. Bipolaron $Nb^{4+}Nb^{4+}$ absorption band in lithium niobate induced by partial reduction.

perature lifetime is from several weeks to several months depending on the reduction state of the material.

Materials Optimization: Fe and Mn Doping

Extrinsic dopants may play essentially the same role as deep bipolarons provided that their energy levels are sufficiently deep in the forbidden gap of the crystal. Because the densities of the deep and shallow traps in undoped crystals cannot be separately controlled by reduction alone, introduction of deep extrinsic levels provides a means to control the concentrations of deep traps. Normally, the ionization absorption for dopants in $LiNbO_3$ is quite broadband, and, therefore, to achieve high gating efficiency, it is important to separate the absorption peaks for deep donors and metastable polarons (~780 nm) as far as possible. Mn^{2+} and Fe^{2+} are appropriate deep donors because their energy levels lie below that of the bipolarons in the forbidden band gap (*6*), and, therefore, one should expect a smaller photoionization cross section for near IR light for these donors compared with bipolarons. Therefore, material improvements obtained in weakly Fe-doped crystals are related to the gating efficiency of the two-photon recording process and hologram lifetime upon continuous readout.

Reduction converts the majority of the extrinsic impurities (such as Fe or Mn ions) into donors (Fe^{2+} and Mn^{2+}; Fig. 6) (*12*). For 0.02 mol % Mn-doped samples, at least 90 to 95% of the Mn ions need to be converted (through reduction) into the Mn^{2+} valence state before any appreciable two-photon response can be detected. The optimum reduction for doped crystals requires stronger reducing conditions compared with undoped crystals. Typical processing conditions involve temperatures of about 950° to 1000°C and durations of about 30 min in a flow of dry pure argon. Similarly to undoped material, stronger reduction of Mn- and Fe-doped crystals gives rise to high dark conductivity and fast grating erasure immediately after recording. The dark decay and IR erasure are further enhanced in crystals doped with Rh and Ti, which have energy levels similar to those of the small polarons in the band gap.

Two reduced Mn^{2+}-doped crystals with 0.01 and 0.03 mol % concentrations were examined and compared with an undoped crystal. Under similar conditions, sensitivities of 0.010, 0.012, and 0.008 cm/J with the gating light of 457.9 nm were observed for the undoped crystal, 0.01 mol % Mn-doped crystal, and 0.03 mol % Mn-doped crystal, respectively. When the gating wavelengths were varied from 457.9 to 514.5 nm, the 0.01 mol % Mn^{2+}-doped crystal exhibited a 10-fold decrease in sensitivity, whereas the undoped crystal showed only a threefold decrease. This difference can be attributed to higher absorption for the blue gating wavelength in Mn:$LiNbO_3$. Because the Mn^{2+} absorption band peaks near 450 nm, the charge excitation from the Mn donors becomes more efficient at shorter wavelengths and causes an enhanced sensitivity in the blue gating region. The decreased sensitivities at 514.5 and 488 nm compared with the undoped reduced crystal may be due to a reduced absorption cross section of Mn^{2+} at this wavelength as compared with that of bipolarons. A decrease in sensitivity by a factor of 2 was seen when the Mn content was increased from 0.01 to 0.03 mol %, which indicates that an optimal doping concentration exists for a high sensitivity and decreased IR erasure rate. The trend with respect to the doping concentration may be due to the decreased lifetime of polarons resulting from an increased effect of direct recombination (tunneling) of carriers from shallow traps to deep donors.

Stoichiometric lithium niobate crystals (Li_2O content of 49.9 mol %) with varying Fe concentrations (*13*) were subjected to reduction processing, and their properties were studied. The sensitivity versus gating intensity at three different gating wavelengths for a lightly doped crystal with 0.01 weight % Fe and 2-mm thickness is shown in Fig. 7A. The saturated sensitivity is similar to that of undoped crystals (with [Li_2O] = 49.6 mol %) (Fig. 7B). An improvement in the sensitivity at 488 and 457 nm occurs compared with that at 514 nm, which is more pronounced for the Fe-doped crystal than for the undoped crystal. This improved sensitivity is due to the Fe^{2+} absorption band centered around 480 nm, where Fe^{2+} has a large ionization cross section.

As in Mn^{2+}, similar sensitivity dependence with doping concentration is observed in Fe-doped crystals, indicating that there also exists an optimal Fe-doping concentration. When the concentration of Fe increases in the crystal, a direct recombination from the small polarons into the Fe^{3+} traps becomes more pronounced (*14*), decreasing the lifetime of the small polaron concentration and thereby decreasing the two-photon sensitivity.

Comparison of Doped and Undoped Material

Comparison of the sensitivity of an Fe-doped and an undoped reduced 49.6 mol % Li_2O crystal (Fig. 7B) shows that the dynamic range of the Fe-doped crystal is about 60% greater than that of the undoped sample with 49.6 mol % Li_2O. This may be due, however, to the fact that the Fe-doped crystal is nearer to the stoichiometric composition. Out of all (doped and undoped) materials studied in our work, the largest dynamic range was found in a lightly reduced undoped material with the smallest defect density (index change $dn \sim 0.6 \times 10^{-3}$ for undoped $LiNbO_3$ with [Li_2O]

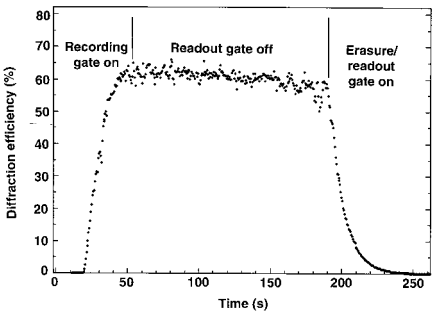

Fig. 5. Gated recording and nondestructive readout in an undoped lightly reduced crystal (Li_2O content 49.6 mol %; IR intensity is 6 W/cm^2). E_{Fermi} is the Fermi level. Open and solid circles denote acceptors and donors, respectively.

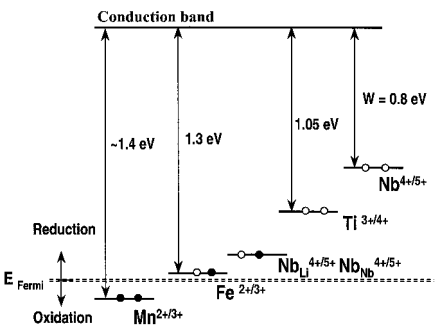

Fig. 6. Relative energy position of different impurities and intrinsic defect centers in the forbidden gap of $LiNbO_3$.

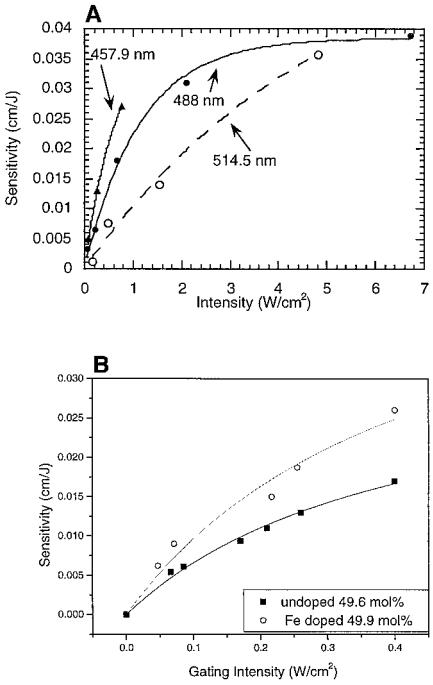

Fig. 7. (**A**) Two-photon sensitivity versus 514.5-, 488-, and 457.9-nm gating light intensity in reduced Fe:$LiNbO_3$ (Li_2O content of 49.9 mol %). Writing intensity is 5 W/cm^2. (**B**) Two-photon sensitivity for reduced stoichiometric Fe-doped and undoped (49.6 mol % Li_2O) $LiNbO_3$ at various 457.9-nm gating intensities. Writing intensity is 10 W/cm^2.

= 49.9 mol %). The undoped crystals of a composition near exact stoichiometry (with 49.9 mol % Li_2O content) have a dynamic range about twice as great as that of a Fe-doped crystal of the same composition (but about three times lower sensitivity). The comparison of the IR erasure of the Fe-doped and the undoped crystals is shown in Fig. 8. The erasure upon continuous IR readout is almost three times slower in a Fe-doped sample compared with that in an undoped crystal with 49.6 mol % Li_2O content and is comparable with that in an undoped 49.9 mol % sample, which, however, has lower (×3) sensitivity than the Fe-doped crystals. This combined effect results in an at least threefold improvement in the gating efficiency in stoichiometric Fe-doped material compared with undoped samples used previously for two-photon recording and storage.

System Issues

To assess the relative performance of these materials, it is necessary to consider the holographic recording system as a whole. Trade-offs need to be made to balance capacity against data transfer rate and signal-to-noise ratio (SNR) or BER. This is best illustrated by considering a basic holographic system layout, shown in Fig. 1. Digital data are input to the system through a spatial light modulator (SLM) and arranged into a two-dimensional pattern for recording in the holographic medium. The pixels in the SLM are arranged in patterns that encode bit groups to allow for error correction and channel coding (*15*). Multiple pages are superimposed inside the medium with angular multiplexing. Further capacity increase is achieved by spatial multiplexing. Upon readout, the pages are recalled by positioning the reference beam at the same orientation as used during recording. The diffracted light from the hologram is detected by a two-dimensional array and decoded into bit streams. The parallelism of detecting all bits in the page simultaneously gives rise to an extremely high data transfer rate. As is the case in conventional storage systems, channel coding is used to reduce the effects of noise, and a target raw BER of 10^{-4} or better is sufficient to achieve a final user BER of less than 10^{-14} with error correction encoding.

The required trade-offs can be captured by considering the following approximate equation:

$$\#\ \text{pages} = \left(\frac{(M/\#)^2 \Theta QEP \eta_{\text{opt}} \eta_{\text{fix}} t_{\text{read}}^2}{MNp_{\text{min}}} \right)^{1/2} \quad (4)$$

where $M/\#$ is a variable based on system and materials parameters, Θ is the number of photons per watt, QE is the quantum efficiency of the detector array, P is the power of the readout beam, η_{opt} is the optical efficiency of the imaging system, η_{fix} is the fixing efficiency, t_{read} is the read time of the recalled data, M and N are the number of pixel rows and columns, respectively, on the data page, and p_{min} denotes the number of photoelectrons needed to get a 20-dB SNR (*16*). It is assumed that bit patterns are balanced (although this does not have to be the case) and half the pixels in a page are on and half are off. From this equation, the trade-off between capacity and data transfer rate is determined. Coding considerations can lower the required SNR, thereby increasing the number of holograms that can be superimposed.

The capacity of the system is proportional to the number of pages per stack, the page size, and the code rate (the number of bits per pixel), whereas the data transfer rate scales as the data page size times the readout rate multiplied by the code rate. As a general construct, the capacity of the storage system is maximized as the number of superimposed pages is maximized. This can be achieved by, for example, increasing $M/\#$. $M/\#$ is dependent on many system and materials parameters but reflects roughly the ratio of the erasure and the recording time constants for plane waves (*17*). For image-bearing waves, the $M/\#$ is strongly dependent on the modulation index of the recordings and is often an order of magnitude smaller than for plane wave recordings and not directly related to the recording and erasure times.

Equation 4 also shows that, for a given $M/\#$, the diffracted signal strength is inversely proportional to the number of superimposed pages squared. To maximize the capacity, the holograms' diffraction efficiency must be kept at its minimum acceptable value. Any absorption during readout of the diffracted signal is undesirable, making gated recording and single-wavelength IR readout more advantageous compared with nongated recording in Fe-doped congruent $LiNbO_3$, which exhibits equal absorption during recording and readout. Besides, two-photon gated recording and single (near IR) wavelength readout produce a large asymmetry in the readout and recording times, as high as a factor of 50 to 1000, thereby largely avoiding information erasure during data readout.

From this trade-off analysis, we note that an ideal material would have a large $M/\#$ and have no absorption and photosensitivity during readout and would be of very high optical quality so that noise scattered into the detector is small. For digital holographic storage, the SNR of the detected signal determines the raw BER. In the limit, if a very large number of superimposed holograms are stored in the medium, cross talk between holograms becomes dominant. In most of our previous work with $LiNbO_3$ doped with iron, we never reached this state of performance, because the dominant noise source is photovoltaic damage. This damage is proportional to the Fe^{3+} concentration as stated above, and in gated recording this effect is much reduced, making it possible to store more holograms and increase capacity.

There is, however, signal-dependent and random noise for compositions close to stoichiometric. From a sensitivity perspective, we would like to be close to stoichiometric, but in that regime crystals are more striated and difficult to grow with good optical quality. Therefore, we try to find a compromise where we get as close to a stoichiometric composition as needed from a sensitivity requirement while compensating for the material inhomogeneities by using a phase conjugate readout beam (Fig. 1). Phase conjugation (*18*) compensates to a large extent for the distortions introduced by the material.

In conclusion, by changing the stoichiometry and the reduction state of photorefractive lithium niobate we achieved a two order of magnitude increase in the two-photon re-

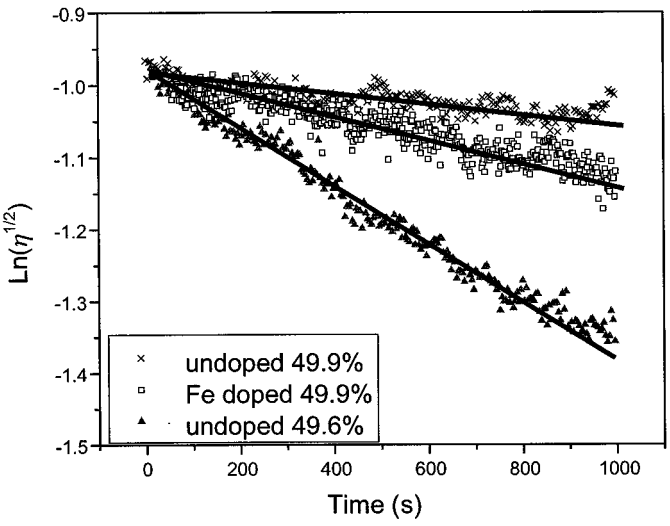

Fig. 8. IR erasure at 790 nm versus time for reduced stoichiometric 49.9 mol % Li_2O Fe-doped and reduced undoped 49.6 mol % [Li_2O] and 49.9 mol % [Li_2O] $LiNbO_3$. IR beam intensity is 5 W/cm^2.

sponse. Small polarons are identified as metastable species responsible for the near IR sensitivity, whereas bound bipolarons play the role of deep donors in undoped material. By introducing deep level dopants, such as Fe^{2+} and Mn^{2+}, in reduced crystals, the gating efficiency and readout erasure time can be increased further compared with undoped material. The dark decay is slower because the deeper donor levels are more resistant to thermal activation of trapped electrons. Other options of dopants include, for example, $Cu^{+/2+}$, whose energy levels lie between Fe and Mn, as well as combinations of dopants, such as Fe and Mn (*19*).

References and Notes

1. J.-P. Huignard and P. Günter, Eds., *Photorefractive Materials and Their Applications*, vol. 61 of *Topics in Applied Physics* (Springer-Verlag, New York, 1988).
2. D. von der Linde, A. M. Glass, K. F. Rodgers, *Appl. Phys. Lett.* **25**, 155 (1974).
3. Y.-S. Bai and R. Kachru, *Phys. Rev. Lett.* **78**, 2944 (1997).
4. D. Lande, S. S. Orlov, A. Akella, L. Hesselink, R. R. Neurgaonkar, *Opt. Lett.* **22**, 1722 (1997).
5. S. S. Orlov, A. Akella, L. Hesselink, R. R. Neurgaonkar, paper presented at the Conference on Lasers and Electro-Optics '97, Optical Society of America, Baltimore, MD, 18 to 23 May 1997.
6. O. F. Schirmer, O. Thiemann, M. Wöhlecke, *J. Phys. Chem. Solids* **52**, 185 (1991).
7. P. Nagels, in *The Hall Effect and its Applications*, C. L. Chien and C. R. Westgate, Eds. (Plenum, New York, 1980), pp. 253–279.
8. Details of the crystal growth, reduction, and the sensitivity measurements are available at www.sciencemag.org/feature/data/976102.shl.
9. A. Garcia-Cabañes *et al.*, *Phys. Rev. B* **37**, 6085 (1988).
10. J. Koppitz, A. I. Kuznetsov, O. F. Schirmer, M. Wöhlecke, B. C. Grabmaier, *Ferroelectrics* **92**, 233 (1989).
11. A. Mehta, E. K. Chang, D. M. Smyth, *J. Mater. Res.* **6**, 851 (1991).
12. The role of reduction for two-photon material response optimization is somewhat different for undoped and doped (with Fe and Mn) crystals (Fig. 6). In undoped crystals, reduction increases the absorption of as-grown material for the gating (blue or green) wavelength because of an increased amount of bipolarons. Optimum reduction steps usually require a processing temperature of about 900°C for a duration of 15 to 30 min (in dry argon). Crystals nearer the stoichiometric composition (49.9 mol % Li_2O) require lighter reducing conditions. Sensitivities up to 0.025 cm/J with an index change of 0.5×10^{-3} can be achieved in the best undoped crystals without postrecording relaxation and with long dark storage times (several days to weeks). Doped crystals, if reduced under conditions optimal for undoped materials, usually exhibit little or almost no two-photon response.
13. Several stoichiometric lithium niobate crystals with varying Fe concentrations grown with a continuous charge double crucible Czochralski method were provided to us by the National Institute for Research in Inorganic Materials in Japan (K. Kitamura).
14. F. Jermann, M. Simon, E. Kratzig, *J. Opt. Soc. Am. B* **12**, 2066 (1995).
15. J. F. Heanue, M. C. Bashaw, L. Hesselink, *Science* **265**, 749 (1994).
16. L. Hesselink, paper presented at the Optical Society of America Annual Meeting, Rochester, NY, 20 to 24 October 1996.
17. F. H. Mok, G. W. Burr, D. Psaltis, *Opt. Lett.* **21**, 896 (1996).
18. B. Y. Zeldovich, N. F. Pilipetsky, V. V. Shkunov, *Principles of Phase Conjugation* (Springer-Verlag, New York, 1985).
19. D. L. Staebler and W. Phillips, *Appl. Phys. Lett.* **24**, 268 (1974).

20. This research is partially funded by the Defense Advanced Research Project Agency-NSIC-Industry-University Photorefractive Information Storage Materials Consortium under contract (MDA972-94-2-008) with L. N. Durvasula as contract monitor. We acknowledge the members of the PRISM consortium for helpful discussions, in particular W. Phillips of Optitek, P. MacFarlane and H. Guenther of IBM Almaden, R. Schwartz from Hughes Research Laboratories, and R. Kachru and Y.-S. Bai of Stanford Research Institute. We thank R. Feigelson of Stanford University at the Center of Materials Research for use of the crystal growth facilities and helpful discussions, K. Kitamura of the National Institute for Research in Inorganic Material, Japan, for providing stoichiometric Fe-doped samples, and D. Quay and L. Galambos for assistance with the crystal growth at Stanford University.

10 November 1997; accepted 17 September 1998

Photorefractive Materials for Nonvolatile Volume Holographic Data Storage

Lambertus Hesselink, Sergei S. Orlov, Alice Liu, Annapoorna Akella, David Lande and Ratnakar R. Neurgaonkar (November 6, 1998)

Science **282** (5391), 1089-1094. [doi: 10.1126/science.282.5391.1089]

Editor's Summary

Science (print ISSN 0036-8075; online ISSN 1095-9203) is published weekly, except the last week in December, by the American Association for the Advancement of Science, 1200 New York Avenue NW, Washington, DC 20005.